Structure determination of Bi/Ge(111)-$(\sqrt{3} \times \sqrt{3})R30^\circ$ by dynamical low-energy electron diffraction analysis and scanning tunneling microscopy

Yoshiyuki Ohtsubo[1,2], Shinichiro Hatta[1,2], Manabu Iwata[1], Koichiro Yaji[1,2], Hiroshi Okuyama[1] and Tetsuya Aruga[1,2]

[1] Department of Chemistry, Graduate School of Science, Kyoto University, Kyoto 606-8502, Japan

[2] JST CREST, Saitama 332-0012, Japan

E-mail: aruga@kuchem.kyoto-u.ac.jp

Abstract. We have determined the atomic structure of the Bi/Ge(111)-$(\sqrt{3} \times \sqrt{3})R30^\circ$ surface by dynamical low-energy electron diffraction (LEED) analysis and scanning tunneling microscopy (STM). The optimized atomic structure consists of Bi atoms which are adsorbed near the T_1 sites of the bulk-truncated Ge(111) surface and form triangular trimer units centered at the T_4 sites. The atomically resolved STM image was consistent with the LEED result. The structural parameters agree well with those optimized by a first-principles calculation which supports the interpretation of the electronic band splitting on this surface in terms of the giant Rashba effect.

PACS numbers: 61.05.jh, 68.37.Ef, 68.47.Fg

Submitted to: *J. Phys.: Condens. Matter*

1. Introduction

Recently, much attention has been paid to the large spin splitting of surface bands due to the Rashba spin-orbit interaction [1, 2]. It has been shown that the large Rashba spin splitting is realized on surfaces of heavy elements such as Au [3] and Bi [4, 5]. The Rashba spin splitting was also observed on substrates of lighter elements, such as Ag, covered with heavy elements [6, 7]. This suggests that the giant Rashba spin splitting is also possible on the surfaces of semiconductors such as Si and Ge, implying a possibility of novel spin transport phenomena on surfaces.

We recently studied the electronic structure of the Bi/Ge(111)-$(\sqrt{3} \times \sqrt{3})R30^\circ$ surface. On this surface, Rashba-like band splitting was observed by angle-resolved photoelectron spectroscopy (ARPES) [8]. The splitting appeared to be quite large compared to those on the Bi surfaces. A theoretical approach based on accurate atomic

structure provides further insight into surface electronic structure and spin splitting [9, 10, 11]. Therefore, the precise structural determination of Bi/Ge(111)-$(\sqrt{3}\times\sqrt{3})R30^\circ$ was indispensable for studying the large spin splitting.

The submonolayer to monolayer (ML) coverages of group-15 elements on semiconductor (111) surfaces lead to various atomic structures. Here, we define 1 ML as the atom density of bulk-truncated Si or Ge(111). The P/Ge(111) [12], Sb/Si(111) [13, 14, 15] and Bi/Si(111) [16, 17, 18, 19] surfaces at 1 ML have the $(\sqrt{3}\times\sqrt{3})R30^\circ$ structure with a common adatom geometry (T_4 trimer). Adatoms adsorb near the T_1 sites of bulk-truncated Si or Ge(111) and form triangular trimer units centered at the T_4 sites. On Bi/Si(111), another type of the $(\sqrt{3}\times\sqrt{3})R30^\circ$ structure (T_4 monomer) is also formed depending on the sample preparation condition. In the T_4 monomer structure, Bi adatoms of 1/3 ML adsorb on every third T_4 site of bulk-truncated Si(111). This structure is similar to those observed on the Si(111) surfaces covered with group-13 elements [20]. On Bi/Ge(111), the T_4 monomer structure was reported in the study based on dynamical LEED analysis [21]. On the other hand, a density-functional-theory (DFT) calculation predicted that the T_4 monomer, T_4 trimer and bare reconstructed Ge(111) structures coexist at coverages below 1/3 ML and that the T_4 trimer structure is the most stable phase at 1 ML [18]. However, the T_4 trimer phase has not been confirmed experimentally.

In this work, we attempted to clarify the atomic structure of the Bi/Ge(111)-$(\sqrt{3}\times\sqrt{3})R30^\circ$ structure by dynamical LEED analysis and scanning tunneling microscopy (STM). The intensity vs voltage (I-V) curves in energy range much wider than in the former work [21] were collected and analysed. The analysis yielded the T_4 trimer structure. The atomically resolved STM image was consistent with this result. The optimized structural parameters show a good agreement with those obtained by the first-principles calculation.

2. Experimental details

Experiments were performed in two separate ultrahigh vacuum chambers, one for STM and the other for LEED. The base pressure was $\sim 1\times10^{-10}$ Torr in the STM chamber and $\sim 2\times10^{-10}$ Torr in the LEED chamber. A variable-temperature STM (Oxford Instruments) with a chemically etched polycrystalline tungsten tip was used. All the STM images were taken in the constant-current (topographic) mode at room temperature.

The Ge(111) samples were sliced from a non-doped single crystal. The clean Ge(111) surface was prepared by repeated cycles of Ar ion sputtering at 750 eV and annealing up to $\sim$950 K until a sharp c(2×8) LEED pattern was obtained as shown in figure 1. Bi was deposited from an alumina crucible heated by a tungsten wire loop with the surface temperature kept at <320 K. Upon Bi deposition, the $c(2\times8)$ pattern gradually disappeared, after which diffuse (2×1), or (2×2), and well-contrasted (1×1) patterns were succeedingly observed [22]. Post-annealing of the (1×1) surface at $\sim$ 700

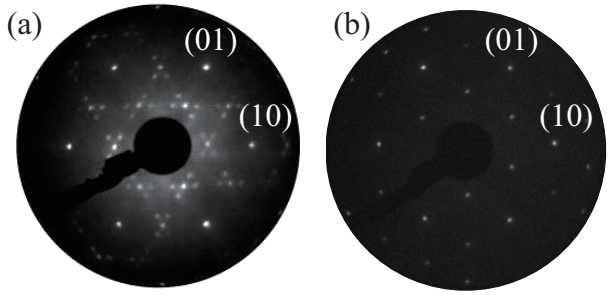

Figure 1. (a) LEED pattern of Ge(111)-c(2×8) at room temperature. (b) LEED pattern of Bi/Ge(111)-($\sqrt{3} \times \sqrt{3}$)$R30°$ at 110 K. (E_p = 144 eV)

K for 5 min resulted in a sharp ($\sqrt{3} \times \sqrt{3}$)$R30°$ LEED pattern as shown in figure 1.

Normal-incidence LEED patterns at 80–450 eV were recorded at 110 K at an interval of 2 eV by a computer-controlled image acquisition system. The I-V curves were normalized to the primary beam current and averaged over the symmetrically equivalent beams according to the plane symmetry group p31m. The obtained data set consisted of seven inequivalent beams [(1 0), (0 1), (1 1), (1/3 1/3), (2/3 2/3), (1/3 4/3), (4/3 1/3)], and had a total energy range of 2296 eV. The I-V curves appear to have characteristics very similar to those reported previously [21].

The Barbieri-Van Hove symmetrized automated tensor LEED (SATLEED) package was used to simulate the I-V curves for different structure models [23]. Crystal potentials for Ge and Bi were described by phase shifts obtained by the Barbieri-Van Hove phase shift package. We used phase shifts up to l_{max}=8 for an initial screening to rule out inadequate models, and up to l_{max}=12 for the optimization of the accurate atomic structure. The calculated and experimental I-V curves were compared by means of the reliability factor defined by Pendry ($R_{\rm P}$) [24]. The thermal effect was taken into account in the calculation by optimizing the Debye temperature for each atomic layer. The errors of the structural parameters were evaluated with the Pendry RR function [24].

The density-functional-theory (DFT) calculations were performed by employing the WIEN2k computer code [25, 26]. This calculation utilizes the full-potential 'augmented plane wave + local orbitals' (APW+lo) method [27, 28] and the PBE96 generalized gradient approximation (GGA) [29] to construct the exchange and correlation potentials. We used a slab geometry consisting of Bi and 10 Ge(111) layers to simulate the Bi/Ge(111)-($\sqrt{3} \times \sqrt{3}$)$R30°$ surface. The Bi atoms were arranged according to several adatom geometries (see figure 2) including the T_4 trimer structure. Then the positions of all Bi and Ge atoms were optimized until the root-mean-square force became smaller than 2 mRy/a.u. (For details about surface electronic structure calculated for this surface structure, see [8]).

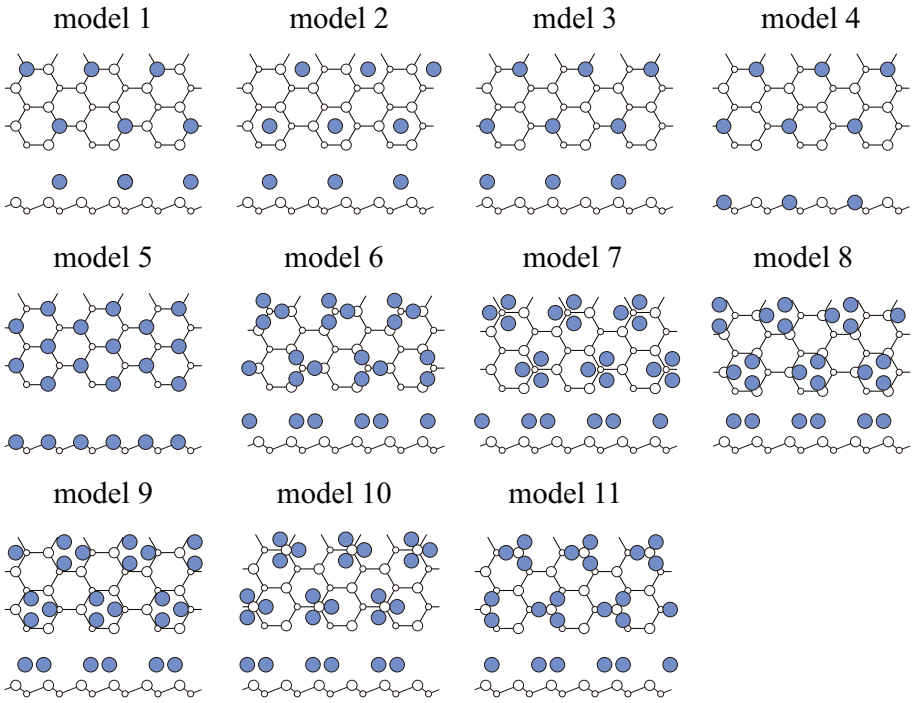

Figure 2. Eleven examined structure models for Bi/Ge(111)-($\sqrt{3} \times \sqrt{3}$)$R30°$. Filled and open circles represent Bi and Ge atoms, respectively.

3. Results and discussion

In dynamical LEED analysis, we examined eleven structure models. The top and side views of these models are shown in figure 2. The Bi coverage is 1/3 ML for models 1–4 and 1 ML for models 5–11. Models 1 and 2 are the same as those examined in the former LEED analysis [21]. In models 1–3, Bi atoms are located on the threefold symmetry sites (T_4, H_3 and T_1, respectively) on the bulk-truncated Ge(111)-(1×1) surface. In models 4 and 5, the topmost Ge atoms of the bulk-truncated surface are replaced with Bi atoms. In model 5, the height variation of neighboring Bi atoms is allowed in the ($\sqrt{3} \times \sqrt{3}$)$R30°$ periodicity. In models 6–11, Bi trimer units are located at T_4 (models 6 and 7), H_3 (8 and 9), and T_1 (10 and 11) sites with different orientations. Models 1 and 6 correspond to the T_4-monomer and T_4-trimer structures, respectively, mentioned above.

We first optimized the atomic positions of Bi and Ge atoms in the first two Ge layers for the eleven models. The displacements were done in the way according to the plane symmetry group p31m. The calculated R_P values for all models are shown in figure 3. Model 6 yielded a notably small R_P value of 0.25. Since the variance of R_P was 0.03, the other models were ruled out. We further optimized the structural parameters of Bi adatoms and the first four Ge layers for model 6. The Debye temperatures for the Bi adatoms and the topmost-layer Ge atoms were also optimized, which yielded 120 K for Bi and 374 K for the first-layer Ge atoms. These were almost the same values as

Table 1. Atomic positions of the T_4 trimer model optimized by dynamical LEED analysis. The errors of first six atoms are in parentheses (Since R_P is not sensitive to atomic positions of deeper atoms, errors of them from Pendry RR function is not significant). N represents the lateral displacements that are zero due to the symmetry.

Atom	x (Å)	y (Å)	z (Å)
1 Bi	1.73 (0.08)	0.00 (N)	0.00 (0.02)
2 Ge	2.28 (0.07)	0.00 (N)	2.69 (0.02)
3 Ge	3.46 (N)	2.00 (N)	3.45 (0.02)
4 Ge	0.00 (N)	0.00 (N)	3.66 (0.04)
5 Ge	3.46 (N)	2.00 (N)	5.91 (0.02)
6 Ge	0.00 (N)	0.00 (N)	6.08 (0.05)
7 Ge	1.17	2.03	6.77
8 Ge	1.15	2.00	9.36
9 Ge	2.30	0.00	10.04
10 Ge	2.32	0.00	12.48
11 Ge	0.00	0.00	13.34
12 Ge	3.46	2.00	13.27

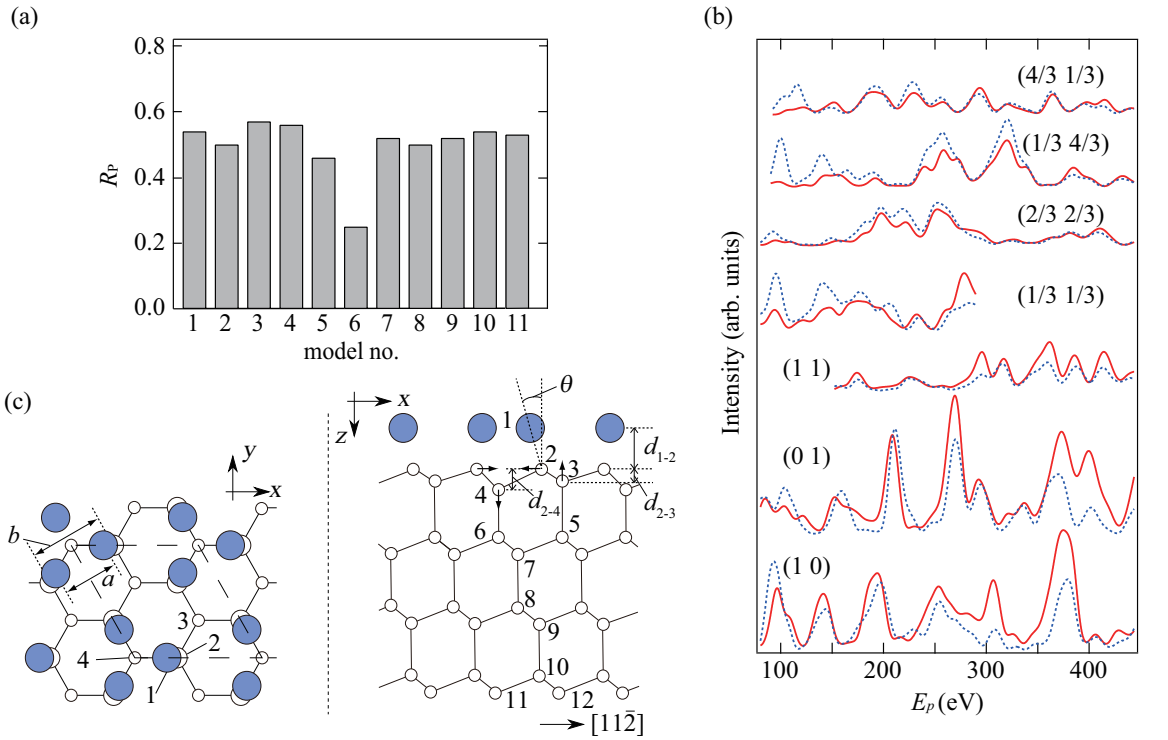

Figure 3. (a) Comparison of R_P for the structure models examined. (b) Comparison of the experimental (full) and calculated (dashed) I-V curves for the optimized T_4 trimer model. (c) Top and side views of the T_4 trimer model. Filled and open circles represent Bi and Ge atoms, respectively.

the bulk values for Bi (119 K) and Ge (374 K). Those for Ge in the deeper layers had been fixed at the bulk value. The imaginary part of the inner potential was fixed at –5

eV. We eventually obtained $R_{\mathrm{P}} = 0.22$. The comparison between the experimental and simulated I-V curves shows a good overall agreement as shown in figure 3.

The optimized atom positions of the T_4 trimer structure (model 6) are listed in table 1. The atom labels of the Bi and Ge atoms correspond to those indicated in figure 3. Figure 4 shows the interatomic distances obtained by the dynamical LEED analysis and the DFT calculation, which shows a good overall agreement. In order to clarify the relaxation from the bulk structure, the bulk nearest-neighbor Bi–Bi and Ge–Ge distances (3.05 and 2.45 Å, respectively) and the average of them (2.75 Å) are indicated by dotted lines.

In order to check if there coexist $(\sqrt{3}\times\sqrt{3})R30°$ phases with different atomic structures, we measured I-V curves at room temperature after the surface covered with 3 ML of Bi was annealed at temperatures from 420 to 770 K in which the $(\sqrt{3}\times\sqrt{3})R30°$ LEED pattern was observed. Annealing above 800 K resulted in the diffuse c(2×8) LEED pattern, indicating the desorption of the Bi adatoms. Since I-V curves are sensitive to surface atomic structure, the peak positions of the I-V curves would change if different $(\sqrt{3}\times\sqrt{3})R30°$ structures with different stability are formed. However, as shown in figure 5, no significant change was observed over the whole temperature range. We also confirmed that the photoelectron intensity of the Bi 5d core level was not changed upon annealing the surface with 1 ML Bi up to 740 K. We conclude that the $(\sqrt{3}\times\sqrt{3})R30°$ surface is monophase under the preparation condition employed. Note that this does not rule out all the possibility of existance of the T_4 monomer. Bi deposition below 1/3 ML before annealing may induce the T_4 monomer structure.

We observed the Bi/Ge(111)-$(\sqrt{3}\times\sqrt{3})R30°$ surface by STM. Figure 6 shows an atomically resolved filled-state STM image. A white parallelogram indicates the $(\sqrt{3}\times\sqrt{3})R30°$ unit cell. The STM image shows protrusions forming a triangular trimer structure as indicated by white dashed circles. These trimers are arranged according to the $(\sqrt{3}\times\sqrt{3})R30°$ periodicity and the observed distance of the protrusions within the

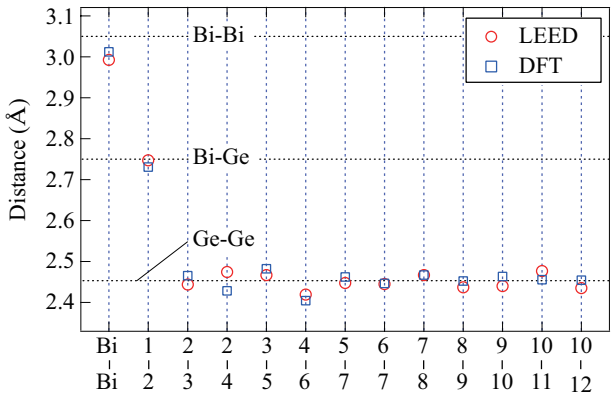

Figure 4. The bond lengths of the T_4 trimer structure optimized by LEED I-V analysis and by the DFT calculation. The atom labels correspond to those in figure 3(c).

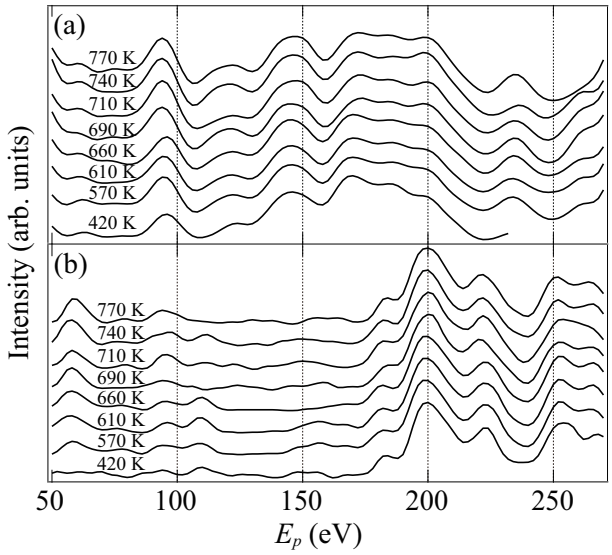

Figure 5. *I-V* curves from (1/3 1/3) (a) and (2/3 2/3) (b) spots. Each *I-V* curve was measured after the deposition of 3 ML Bi followed by annealing for 5 min at indicated temperatures.

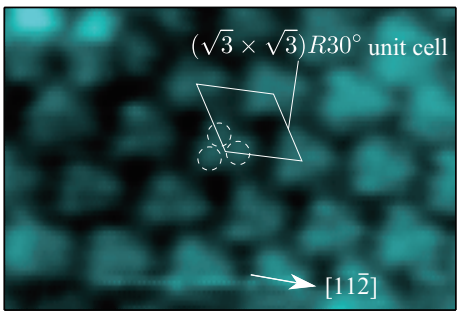

Figure 6. Atomically resolved STM image for Bi/Ge(111)-($\sqrt{3} \times \sqrt{3}$)$R30°$ (28×42 Å^2) at room temperature. V_s= -50.0 mV, I_t= 2.00 nA.

trimers is 2.8 ± 0.3 Å, which is in agreement with the trimer structure as optimized by the LEED *I-V* analysis and the DFT calculation.

The characteristic structural parameters of the Bi/Ge(111)-($\sqrt{3} \times \sqrt{3}$)$R30°$ surface are compared in table 2 with those for the T_4 trimer structures on Sb/Si(111) and Bi/Si(111) surfaces. On Bi/Ge(111), the Bi–Bi distance in a timer unit is 2.99 Å. This value is very close to the nearest-neighbor distance in bulk Bi, 3.05 Å, as is that in the Bi/Si(111)-($\sqrt{3} \times \sqrt{3}$)$R30°$-β surface [16, 17, 18]. On the Sb/Si(111)-($\sqrt{3} \times \sqrt{3}$)$R30°$ surface [14, 15], the corresponding value is also close to the nearest-neighbor distance in bulk Sb crystal. The local bonding geometry of the adatom in the T_4 trimer structure resembles the bulk structure: In bulk Bi and Sb crystals, atoms are bonded to three nearest-neighbor atoms with bond angles near 90°, which is in agreement with the p^3-like hybridization of Bi and Sb atoms.

Because the Bi–Bi (Sb–Sb) distances in the trimer is shorter than the nearest

Table 2. Characteristic structural parameters for the T_4 trimer structure on the Si(111) and Ge(111) surfaces. (See figure 3 for the definition.)

Surface	a (Å)[a]	b (Å)[b]	θ	d_{1-2} (Å)	d_{2-3} (Å)[c]	d_{2-4} (Å)[c]	References
Sb/Si(111)	2.92	3.63	9.5°	2.44	0.87	0.95	[14]
	2.94	3.57	8°	2.55	0.62	0.90	[15]
Bi/Si(111)	3.05	3.74	8.5°	2.64	0.69	0.87	[18]
Bi/Ge(111)	2.99	3.95	12°	2.75	0.76	0.97	This work (LEED)
	3.01	3.88	11°	2.68	0.76	0.94	This work (DFT)

[a] Bulk nearest-neigbor distance is 2.90 Å for Sb and 3.05 Å for Bi.
[b] Distance on the ideal (1×1) surface is 3.84 Å for Si and 4.00 Å for Ge.
[c] Bulk distance is 0.78 Å for Si and 0.82 Å for Ge.

neighbor Ge–Ge (Si–Si) ones in the topmost layer, the trimer formation induces lattice strain in the substrate. In the topmost Ge layer, outer Ge(2) atoms are horizontally displaced toward the T_4 site. On Sb/Si(111), the horizontal displacements of Si atoms are larger, due probably to the shorter Sb–Sb distance as compare to Bi–Bi. On the other hand, the second-layer Ge(3,4) atoms make vertical relaxations: The Ge(4) atom beneath the Bi trimer is moved downward and the other Ge(3) upward. Because of the trimer formation, Bi(1)–Ge(2) bond is tilted by 11.5° from the surface normal. The relaxation in the topmost Ge bilayer keeps the bond angles 1–2–3 (101.5°), 1–2–4 (113.7°), and 3–2–4 (108.8°) close to that for the sp^3 hybridized orbital (109.5°). The same tendency is observed on the other T_4 trimer surfaces and thus the strain induced by the Bi-trimer formation is efficiently relaxed. Note also that each surface atom has a number of the nearest-neighbor atoms equal to those in their bulk crystals (three for Bi and four for Ge). This is probably why the Debye temperatures of all atoms remains the bulk values.

In spite of the similarity of the I-V curves, the structure obtained for the Bi/Ge(111)-($\sqrt{3} \times \sqrt{3}$)$R30^\circ$ surface is different from that reported previously [21]. This probably comes from the variety of the examined structural models. We believe that if the previous authors had calculated I-V curves for the T_4 trimer structure, it would have shown a better agreement than that for the T_4 monomer structure. In both experimental works, Bi above 1 ML was deposited on clean Ge(111) before preparing ($\sqrt{3} \times \sqrt{3}$)$R30^\circ$ surfaces by annealing. Therefore, the result does not conflict with that of the former DFT calculations [18] that predicted the T_4 trimer structure to be the stable structure at 1 ML.

4. Conclusion

We determined the atomic structure of the Bi/Ge(111)-($\sqrt{3} \times \sqrt{3}$)$R30^\circ$ surface by means of the dynamical LEED analysis and STM. The optimized structure consists of triangle Bi trimer units on T_4 sites of bulk-truncated Ge(111) surface. The local bonding geometry of Bi is similar to that in bulk Bi crystal. There remain no dangling

bonds and the interatomic distances of surface atoms are close to that in the bulk crystals. In the DFT calculation [8] based on the structure optimized in this work, large spin splitting due to the Rashba spin-orbit interaction is found in the occupied states having a significant contribution of the Bi 6s and 6p orbitals, which is consistent with the ARPES result.

Acknowledgments

The authors acknowledge the support by the Global COE Program "Integrated Materials Science" (No. B-09).

References

[1] Rashba E I 1960 *Sov. Phys.–Solid State* **2** 1109
[2] Bychkov Y A and Rashba E I 1984 *JETP Lett.* **39** 78
[3] LaShell S, McDougall B A and Jensen E 1996 *Phys. Rev. Lett.* **77** 3419
[4] Koroteev Yu M, Bihlmayer G, Gayone J E, Chulkov E V, Blügel S, Echenique P M and Hofmann Ph 2004 *Phys. Rev. Lett.* **93** 046403
[5] Hofmann Ph 2006 *Prog. Surf. Sci.* **81** 191-245
[6] Nakagawa T, Ohgami O, Saito Y, Okuyama H, Nishijima M and Aruga T 2007 *Phys. Rev.* B **75** 155409
[7] Ast C R, Henk J, Ernst A, Moreschini L, Falub M C, Pacilé D, Bruno P, Kern K and Grioni M 2007 *Phys. Rev. Lett.* **98** 186807
[8] Hatta S, Ohtsubo Y, Okuyama H and Aruga T 2009 *submitted*
[9] Hatta S, Kato C, Tsuboi N, Takahashi S, Harasawa A, Okuda T, Kinoshita T, Okuyama H and Aruga T 2007 *Phys. Rev.* B **76** 075427
[10] Hatta S, Kato C, Takahashi S, Harasawa A, Okuda T, Kinoshita T, Okuyama H and Aruga T 2008 *Phys. Rev.* B **77** 245236
[11] Hatta S, Ohtomo R, Kato C, Sakata O, Okuyama H and Aruga T 2008 *J. Phys.: Condens. Matter* **20** 395226
[12] Vitali L, Ramsey M G and Netzer F P 2001 *Phys. Rev.* B **63** 165320
[13] Mårtensson P, Meyer G, Amer N M, Kaxiras E and Pandey K C 1990 *Phys. Rev.* B **42** 7230
[14] Kim C, Walko D A and Robinson I K 1997 *Surf. Sci.* **388** 242
[15] Bengió S, Martin M, Avila J, Asensio M C and Ascolani H 2002 *Phys. Rev.* B **65** 205326
[16] Wan K J, Guo T, Ford W K and Hermanson J C 1991 *Phys. Rev.* B **44** 3471
[17] Nakatani S, Takahashi T, Kuwahara Y and Aono M 1995 *Phys. Rev.* B **52** R8711
[18] Cheng C and Kunc K 1997 *Phys. Rev.* B **56** 10283
[19] Schmidt T M, Miwa R H and Srivastava G P 2004 *Brazilian Journal of Physics* **34** 629
[20] LaFemina J P 1992 *Surf. Sci. Rep.* **16** 138 and references therein
[21] Wan K J, Ford W K, Lapeyre G J and Hermanson J C 1991 *Phys. Rev.* B **44** 6500
[22] Hatta S, Ohtsubo Y, Miyamoto S, Okuyama H and Aruga T 2009 Epitaxial growth of Bi thin films on Ge(111) *Appl. Surf. Sci.* (*Preprint VASSCAA-4 proceedings*)
[23] Barbieri A and Van Hove M A *Symmetrized automated tensor leed (SATLEED) package* (available from M. A. Van Hove, http://electron.lbl.gov/vanhove.html)
[24] Pendry J B 1980 *J. Phys.* C **13** 937
[25] Blaha P, Schwarz K, Madsen G K H, Kvasnicka K and Luitz J 2001 *WIEN2k, An Augmented Plane Wave + Local Orbital Program For Calculating Crystal Properties* Karlheinz Schwarz, Technical Universitat Wien, Wien, Austria
[26] Schwarz K, Blaha P and Madsen G K H 2001 *Comput. Phys. Commun.* **147** 71

[27] Sjöstedt E, Nordström L and Singh D J 2000 *Solid State Commun.* **114** 15
[28] Madsen G K H, Blaha P, Schwarz K, Sjöstedt E and Nordström L 2001 *Phys. Rev.* B **64** 195134
[29] Perdew J P, Curke K and Ernzerhof M 1996 *Phys. Rev. Lett.* **77** 3865